

# Numerical analysis of transmission coefficient, LDOS, and DOS in superlattice nanostructures of cubic $\text{Al}_x\text{Ga}_{1-x}\text{N}/\text{GaN}$ resonant tunneling MODFETs

D. Bouguenna<sup>1,2</sup> · T. Wecker<sup>3</sup> · D. J. As<sup>3</sup> · N. Kermas<sup>4</sup> · A. Beloufa<sup>1</sup>

© Springer Science+Business Media New York 2016

**Abstract** Numerical analysis of the transmission coefficient, local density of states, and density of states in superlattice nanostructures of cubic  $\text{Al}_x\text{Ga}_{1-x}\text{N}/\text{GaN}$  resonant tunneling modulation-doped field-effect transistors (MODFETs) using nextnano<sup>3</sup> software and the contact block reduction method is presented. This method is a variant of non-equilibrium Green's function formalism, which has been integrated into the nextnano<sup>3</sup> software package. Using this formalism in order to model any quantum devices and estimate their charge profiles by computing transmission coefficient, local density of states (LDOS) and density of states (DOS). This formalism can also be used to describe the quantum transport limit in ballistic devices very efficiently. In particular, we investigated the influences of the aluminum mole fraction and the thickness and width of the cubic  $\text{Al}_x\text{Ga}_{1-x}\text{N}$  on the transmission coefficient. The results of this work show that, for narrow width of 5 nm and low Al mole fraction of  $x = 20\%$  of barrier layers, cubic  $\text{Al}_x\text{Ga}_{1-x}\text{N}/\text{GaN}$  superlattice nanostructures with very high density of states of  $407\text{eV}^{-1}$  at the resonance energy are

preferred to achieve the maximum transmission coefficient. We also calculated the local density of states of superlattice nanostructures of cubic  $\text{Al}_x\text{Ga}_{1-x}\text{N}/\text{GaN}$  to resolve the apparent contradiction between the structure and manufacturability of new-generation resonant tunneling MODFET devices for terahertz and high-power applications.

**Keywords** Transmission coefficient · Density of states · Local density of states · Cubic  $\text{Al}_x\text{Ga}_{1-x}\text{N}/\text{GaN}$  · Superlattice · Nanostructures · MODFETs · nextnano<sup>3</sup>

## 1 Introduction

In modern physics, the most important field of research is dimensionality reduction for electronic devices such as modulation-doped field-effect transistors (MODFETs), which may enable higher transfer rates in data communication systems [1]. Recently, research interest in group III nitrides has greatly increased, especially in the fields of THz devices, fast modulators, photodetectors [2], and transistors (MODFETs), being the most suitable for use in high-power and high-frequency devices [3]. However, MODFETs with  $\text{Al}_x\text{Ga}_{1-x}\text{N}/\text{GaN}$  in metastable cubic phase represent an alternative to devices based on stable hexagonal III-N nitrides for such applications. Due to the absence of spontaneous and piezoelectric fields, cubic  $\text{Al}_x\text{Ga}_{1-x}\text{N}/\text{GaN}$  facilitates fabrication of field-effect transistors with both normally-on and normally-off characteristics [4].  $\text{Al}_x\text{Ga}_{1-x}\text{N}/\text{GaN}$  structures are limited by a combination of effects such as dislocations and the presence of many structural defects in the bulk, surface, and interface of materials, thus degrading the electric performance of such transistors [5].

Moreover, growth of heterostructures results in formation of a two-dimensional electron gas (2DEG) at the

✉ D. Bouguenna  
dbouguenna.um@gmail.com; driss.bouguenna@univ-usto.dz

<sup>1</sup> Laboratory of Materials, Applications and Environment, Department of Technical Sciences, Faculty of Technology, University Mustapha Stambouli of Mascara, 29000 Mascara, Algeria

<sup>2</sup> Département de l'Électronique, Faculté de Génie Électrique, Université des Sciences et de la Technologie d'Oran Mohamed Boudiaf USTO-MB, BP 1505, El M'naouer, 31000 Oran, Algeria

<sup>3</sup> Department of Physics, University of Paderborn, 33098 Paderborn, Germany

<sup>4</sup> Laboratory of Modelization and Calculation Methods, Department of Electronic, University Dr Moulay Tahar of Saida, 20000 Saida, Algeria

heterointerface. This feature allows for ultrafast, high-efficiency electron and data transport. These outstanding electronic features are attributed to the characteristic density of states in such low-dimensional systems. On the other hand,  $\text{Al}_x\text{Ga}_{1-x}\text{N}/\text{GaN}$  MODFETs have recently attracted major interest for use in electronic devices, particularly for high-power and high-frequency amplifiers. This is motivated by their potential for use in military and commercial applications, e.g., in communication systems, wireless stations, radar systems, high-temperature electronics, and high-power solid-state switching. Currently, state-of-the-art MODFETs are fabricated on *c*-plane wurtzite  $\text{Al}_x\text{Ga}_{1-x}\text{N}/\text{GaN}$  heterostructures. Their inherent polarization fields produce extraordinarily large sheet carrier concentrations at the  $\text{Al}_x\text{Ga}_{1-x}\text{N}/\text{GaN}$  heterointerface, which are advantageous for normally-on-type transistors [6–8].

The contact block reduction (CBR) method aims to find the related Green’s function for ballistic quantum transport in the device; it has been integrated into the *nextnano*<sup>3</sup> package [9]. It can be used to calculate the electronic properties of open quantum systems, such as the transmission coefficient and local density of states. The increasing demands for high-performance computing from end-users are constantly driving improvements in device technology in terms of speed and power. Over the past few decades, scaling of device dimensions has proven to be an effective strategy to decrease power consumption. There is a terminal device making use of resonant tunneling, which has generated considerable interest because of its potential applications in high-speed/frequency, high-power applications, and for novel logic circuits. The current transport in all of these devices is controlled by the resonant tunneling transport phenomenon. The basic approach for realization of such devices involves use of superlattice nanostructures in one of the terminals of a MODFET. It is very difficult to carry out accurate theoretical analysis of such devices to predict their performance. Preliminary results on a field-effect transistor (FET) or unipolar transistor were published by Haddad et al. [10–16].

The tunneling transport phenomenon in quantum devices offers picosecond switching speeds and hence the possibility of designing very high-speed circuits. Based on the continuing improvements in process technology for resonant tunneling devices and the integration of such devices with conventional devices [16–18], it is possible that new devices such as the resonant tunneling MODFET based on cubic  $\text{Al}_x\text{Ga}_{1-x}\text{N}/\text{GaN}$  superlattice nanostructures might establish a niche as next-generation devices for use in terahertz (THz) and high-power applications.

We present herein an investigation of the effect of the width of the barrier layers in superlattice nanostructures. The transmission coefficient was determined for different aluminum mole fractions in the cubic  $\text{Al}_x\text{Ga}_{1-x}\text{N}$  barrier layers in superlattice nanostructures of cubic  $\text{Al}_x\text{Ga}_{1-x}\text{N}/\text{GaN}$  with

barrier layer width of 5 nm and without bias, and we also calculated the local density of states of cubic  $\text{Al}_x\text{Ga}_{1-x}\text{N}/\text{GaN}$  superlattice nanostructures. All results presented in the figures herein can be reproduced using the *nextnano*<sup>3</sup> software, which is provided as an online resource.

## 2 Theoretical analysis

The standard Schrödinger equation for each of the superlattice nanostructures can be written as follows [19]:

In the barrier cubic  $\text{Al}_x\text{Ga}_{1-x}\text{N}$ , we have

$$\partial^2\psi(x)/\partial x^2 + \left(8m^*\pi^2/h^2\right)(E - V)\psi(x) = 0. \quad (1)$$

In the well cubic GaN, we have

$$\partial^2\psi(x)/\partial x^2 + \left(8m^*\pi^2/h^2\right)E\psi(x) = 0. \quad (2)$$

For proper confinement of the electrons in the well, the electron energy  $E$  must be less than the barrier potential  $V$ . The cubic  $\text{Al}_x\text{Ga}_{1-x}\text{N}/\text{GaN}$  superlattice nanostructure resonant tunneling MODFET with three wells considered in the theoretical analysis is shown in Fig. 1. The general solutions of the Schrödinger equation that we consider for this superlattice nanostructure are as follows:

$$\begin{aligned} \psi(x) &= A_1 \exp(kx) + B_1 \exp(-kx), & 0 \leq x \leq x_1. \\ \psi(x) &= A_2 \sin(qx) + B_2 \cos(-qx), & x_1 \leq x \leq x_2. \\ \psi(x) &= A_3 \exp(kx) + B_3 \exp(-kx), & x_2 \leq x \leq x_3. \\ \psi(x) &= A_4 \sin(qx) + B_4 \cos(-qx), & x_3 \leq x \leq x_4. \\ \psi(x) &= A_5 \exp(kx) + B_5 \exp(-kx), & x_4 \leq x \leq x_5. \end{aligned}$$

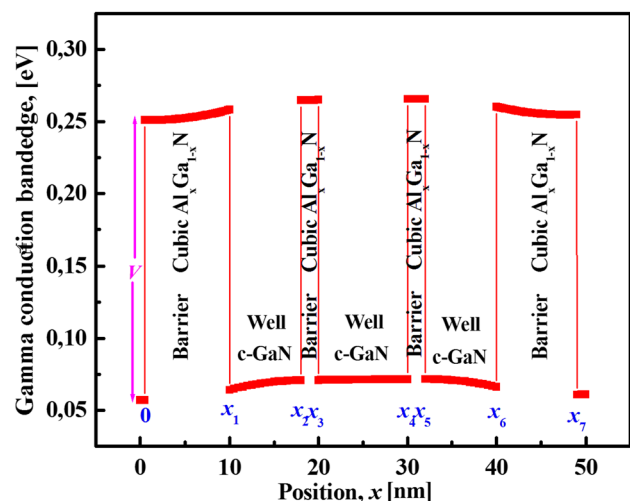


**Fig. 1** Superlattice nanostructures of cubic  $\text{Al}_x\text{Ga}_{1-x}\text{N}/\text{GaN}$  consisting of three wells for resonant tunneling MODFETs with solutions

$$\begin{aligned} \psi(x) &= A_6 \sin(qx) + B_6 \cos(-qx), \quad x_5 \leq x \leq x_6. \\ \psi(x) &= A_7 \exp(kx) + B_7 \exp(-kx), \quad x_6 \leq x \leq x_7. \end{aligned} \quad (3)$$

Here,  $k$  and  $q$  are the wavevectors in barrier region and quantum well, respectively, also being defined as

$$k^2 = \left(8m^*\pi^2/h^2\right) (E - V) \text{ and } q^2 = \left(8m^*\pi^2/h^2\right) E.$$

Using the transfer matrix technique (TMT), the final equation for the superlattice nanostructure can be expressed as

$$\begin{pmatrix} A \\ B \end{pmatrix} = M_1^{-1} M_2 M_3^{-3} M_4 M_5^{-5} M_6 M_7^{-7} M_8 M_9^{-9} M_{10} M_{11}^{-11} M_{12} \begin{pmatrix} K \\ L \end{pmatrix} \quad (4)$$

$$\text{or } \begin{pmatrix} A \\ B \end{pmatrix} = M_S \begin{pmatrix} K \\ L \end{pmatrix}, \quad (5)$$

where  $(A, B)$  and  $(K, L)$  are the coefficients of the matrices for the wavefunction profiles of the respective layers of contact, and  $M_S$  is known as the system matrix.

Equation (5) can be written as

$$\begin{pmatrix} A \\ B \end{pmatrix} = \begin{pmatrix} M_{11} & M_{12} \\ M_{21} & M_{22} \end{pmatrix} \begin{pmatrix} K \\ L \end{pmatrix}. \quad (6)$$

The transmission coefficient can be expressed as the ratio between the flux incident from the left side of the barrier layer cubic  $\text{Al}_x\text{Ga}_{1-x}\text{N}$  and the flux transmitted to the right side, in the absence of any incident wave from the left.

We assume that there are no further nanostructures to the right of the structure, so that no further reflections can occur and the wavefunction beyond the structure can only have a traveling wave component moving to the right; i.e., the coefficient  $L$  must be zero. Thus, Eq. (4) can be modified to

$$\begin{pmatrix} A \\ B \end{pmatrix} = M_S \begin{pmatrix} K \\ 0 \end{pmatrix}. \quad (7)$$

Hence, the transmission coefficient can be obtained from the following expression:

$$T(E) = \frac{1}{M_{11}^* M_{11}}, \quad (8)$$

where  $M_{11}$  is the first matrix element, which is taken from the system matrix  $M_S$ , and  $M_{11}^*$  is the conjugate of  $M_{11}$ .

To study electron tunneling through the superlattice nanostructure, the transmission coefficient is required. The transmission coefficient is considered an important quantity, as it provides most of the relevant information regarding the

transport process in superlattice nanostructures and is characterized by a series of resonance peaks at specific incidence energies.

Recently, modulation-doped cubic  $\text{Al}_x\text{Ga}_{1-x}\text{N}/\text{GaN}$  superlattice nanostructures or quantum wells, with mean free paths and phase-relaxation lengths of several micrometers, have been investigated. The current in any device can be calculated via the transmission function as long as the propagation of electrons through the device is coherent. Coherent propagation means that there are no phase-breaking scattering processes involved. Elastic scattering processes can be taken into account within the contact block reduction (CBR) method if they can be directly included in the Hamiltonian  $H^0$  of the closed system. In this work, we performed calculations of the transmission coefficient and local density of states for resonant tunneling superlattice nanostructures using the CBR method [20] and `nextnano`<sup>3</sup>.

### 2.1 Contact block reduction (CBR) method

CBR is an efficient method that uses a limited set of eigenstates of the decoupled device and a few propagating lead modes to calculate the retarded Green's function of the device coupled to external contacts. From this Green's function, the density and current are obtained in the ballistic limit using Landauer's formula with fixed Fermi levels for the leads [21,22].

The CBR method was first suggested by Mamaluy et al. and has received great attention in recent years due to its ability to compute the retarded Green's function for open systems. The CBR method has been integrated into the `nextnano`<sup>3</sup> software package. It has also been extended to more sophisticated band-structure models, such as the  $\mathbf{k} \cdot \mathbf{p}$  method, to describe hole transport in quantum wires and to tight-binding methods [23]. It can be used to calculate the electronic properties of open quantum systems such as the transmission coefficient and local density of states for correct modeling of nanoscale device behavior [24].

### 3 Device simulation results

We carried out detailed analysis of superlattice nanostructures with thickness of the barrier layers and well width on the order of nanometers. In this work, we used the CBR method to calculate the transmission coefficient and local density of states as functions of barrier layer width and aluminum mole fraction, as well as to calculate the density of states  $D(E)$  for different barrier layer widths of superlattice nanostructures with cubic  $\text{Al}_x\text{Ga}_{1-x}\text{N}/\text{GaN}$  using `nextnano`<sup>3</sup>.

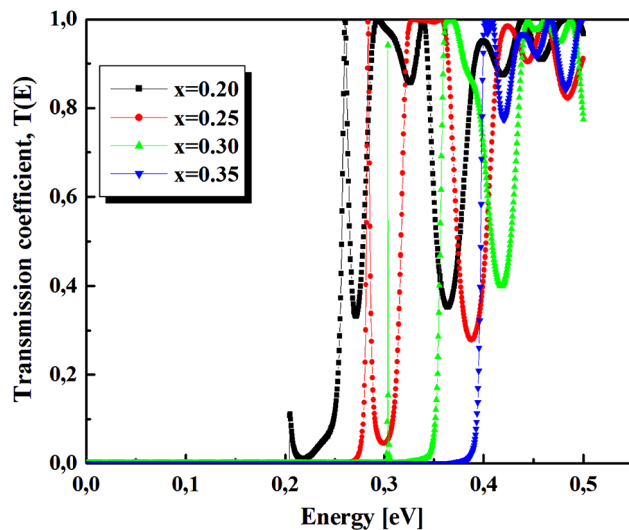


**Fig. 2** Transmission coefficient as function of energy for different Al mole fractions of superlattice nanostructure of cubic  $\text{Al}_x\text{Ga}_{1-x}\text{N}/\text{GaN}$

### 3.1 Results and discussion

The tunneling effect can be analyzed through the transmission coefficient. Determination of the transmission coefficient for eigenstates through the Schrödinger equation for a range of energy permits one to reduce the region of search. Hence, we analyzed the transmission coefficient for different Al mole fractions and barrier widths. The transmission coefficient for different Al mole fractions is depicted in Fig. 2.

#### 3.1.1 Transmission coefficient as function of cubic $\text{Al}_x\text{Ga}_{1-x}\text{N}/\text{GaN}$ superlattice nanostructure

Figure 2 shows the transmission coefficient profile versus electron energy for varying Al mole fraction in the cubic  $\text{Al}_x\text{Ga}_{1-x}\text{N}$  barrier layers for 5 nm width, without bias, and for a specified dimension. With increasing Al mole fraction, the barrier height increases and the mismatch between the effective masses of the superlattice nanostructures becomes more pronounced. This reduces the tunneling probability, as expected. As the Al mole fraction is decreased from 0.35 to 0.2 in steps of 0.05, the probability of electron transmission from the cubic GaN layer through the barrier cubic  $\text{Al}_x\text{Ga}_{1-x}\text{N}$  increases. The maximum tunneling probability occurs when the Al mole fraction in the barrier layers of the cubic  $\text{Al}_x\text{Ga}_{1-x}\text{N}/\text{GaN}$  superlattice nanostructure assumes a value of  $x = 0.2$ .

Figure 3 presents the transmission coefficient calculated as a function of energy for superlattice nanostructures consisting of three wells with varying barrier width of 2, 5, and 10 nm of the cubic  $\text{Al}_x\text{Ga}_{1-x}\text{N}$  layers (barrier height 250 meV, barrier separation 10 nm, grid spacing 0.5 nm, device length 50 nm). At 25 meV, there is a peak where the double super-

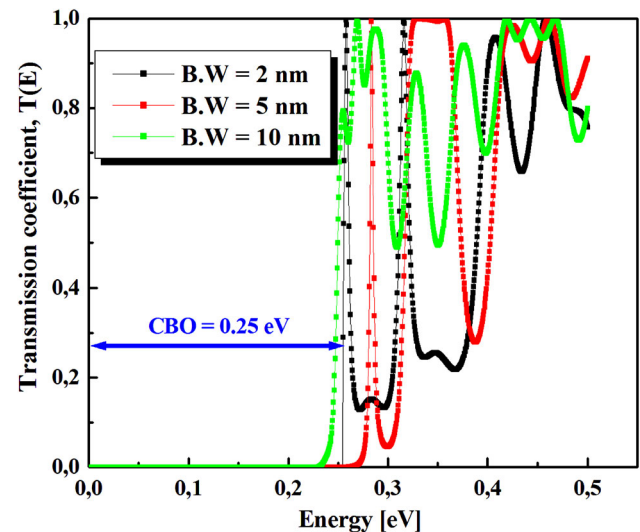


**Fig. 3** Calculated transmission coefficient  $T(E)$  as function of energy for superlattice nanostructure with varying barrier layer widths of 2, 5, and 10 nm of cubic  $\text{Al}_x\text{Ga}_{1-x}\text{N}$  layers (barrier height 250 meV, barrier separation 10 nm)

lattice nanostructure becomes transparent, i.e.,  $T(E) = 1$ . This is exactly the energy that matches the resonant state in the wells. The inset shows the conduction band edge profile and probability density of this quasi-band resonant state for the case of 10-nm barrier width, where the resonant state becomes hardly coupled to the two leads. Figure 3 shows the transmission coefficient  $T(E)$  calculated as a function of energy for this potential profile.

The red line shows  $T(E)$  for barrier height of conduction-band offset (CBO) = 0.25 eV.

#### 3.1.2 Local density of states $\rho(z, E)$ for superlattice nanostructures of cubic $\text{Al}_x\text{Ga}_{1-x}\text{N}/\text{GaN}$

Figure 4 shows the local density of states (LDOS)  $\rho(z, E)$  calculated for superlattice nanostructures as a function of position and energy for the 2- and 5-nm cases. Red (blue) color indicates high (low) density of states. This is in contrast to the situation for the 10-nm barriers (not shown), where due to the large barrier width, the resonance state is quasi-bound, i.e., with very sharp and high density of states at the resonance energy, because of the very weak coupling to the contacts. The reason why we used an energy grid spacing of 0.5 meV is that, if the energy grid is not fine enough, very sharp resonances may be missed in the numerical calculations. However, this grid spacing is still not fine enough to obtain a perfect transmission coefficient ( $T = 1$ ) for the first peak of the superlattice nanostructure with cubic  $\text{Al}_x\text{Ga}_{1-x}\text{N}/\text{GaN}$  with width of 5 nm. Only if the energy grid point exactly matches the resonance energy will the peak be



**Fig. 4** Calculated local density of states of states  $\rho(z, E)$  for superlattice nanostructures of cubic  $\text{Al}_x\text{Ga}_{1-x}\text{N}/\text{GaN}$  resonant tunneling MODFETs as function of position and energy for the **a** 2-nm, **b** 5-nm, and **c** 10-nm cases. Red (blue) color indicates high (low) density of state values (Color figure online)

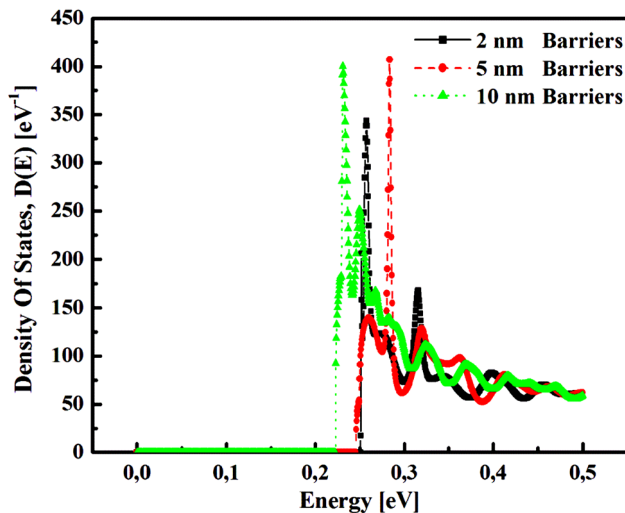
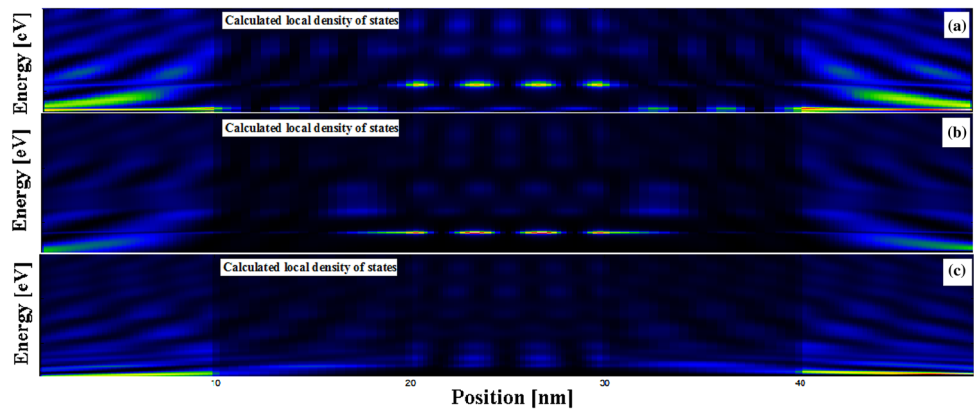


**Fig. 5** Density of states  $D(E)$  calculated for superlattice nanostructures of cubic  $\text{Al}_x\text{Ga}_{1-x}\text{N}/\text{GaN}$  resonant tunneling MODFETs as function of energy

well resolved. This is exactly the energy that matches the resonant state in the wells of the superlattice nanostructure of cubic  $\text{Al}_x\text{Ga}_{1-x}\text{N}/\text{GaN}$ . The LDOS around the resonant state broadens, leading to broadening of the peaks in the transmission coefficient.

### 3.1.3 Density of states $D(E)$ for superlattice nanostructures of cubic $\text{Al}_x\text{Ga}_{1-x}\text{N}/\text{GaN}$

The calculated values of the density of states (DOS) for different barrier widths of 2, 5, and 10 nm for superlattice nanostructures of cubic  $\text{Al}_x\text{Ga}_{1-x}\text{N}/\text{GaN}$  resonant tunneling MODFETs are shown in Fig. 5. In Fig. 5, one observes that, for the 5- and 10-nm barrier widths of cubic  $\text{Al}_x\text{Ga}_{1-x}\text{N}$ , the peak values in the density of states reach  $407$  and  $400 \text{ eV}^{-1}$ , respectively, at Al mole fractions of  $x = 0.28$  and  $0.23$ , respectively. The DOS corresponds to the LDOS integrated over position. The 5-nm case differs substantially from the

other two structures because it is extremely sharp and high. It is actually much higher than the figure suggests, because its maximum is not included on this scale. The third peak in the density of states at  $407 \text{ eV}^{-1}$ , as indicated with red color in Fig. 5 with very high density of states at the resonance energy due to the first confined well state, is only visible for the 5-nm barrier layer width of the cubic  $\text{Al}_x\text{Ga}_{1-x}\text{N}$  nanostructure. This is consistent with the transmission coefficient showing a sharp maximum only for the 5-nm barrier layer width of the cubic  $\text{Al}_x\text{Ga}_{1-x}\text{N}$  nanostructure.

## 4 Conclusions

We present a numerical analysis of the transmission coefficient and local density of states in cubic  $\text{Al}_x\text{Ga}_{1-x}\text{N}/\text{GaN}$  superlattice nanostructures, calculated using the contact block reduction (CBR) method. The effects of the aluminum mole fraction and barrier width of the superlattice nanostructure were simulated using nextnano<sup>3</sup> software. The results illustrate that, for thin width of 5 nm and low Al mole fraction of  $x = 20\%$ , the superlattice nanostructure with cubic  $\text{Al}_x\text{Ga}_{1-x}\text{N}/\text{GaN}$ , having a very high density of states of  $407 \text{ eV}^{-1}$  at the resonance energy, is preferred to achieve the maximum transmission coefficient, as also deduced by considering the tunneling effect. This analysis is very useful for studying the performance of cubic  $\text{Al}_x\text{Ga}_{1-x}\text{N}/\text{GaN}$  superlattice nanostructure resonant tunneling MODFETs, promising a viable means of dramatically improving the performance and density of states of future devices, especially for use in the fields of THz and high-power applications. Based on ongoing improvements in process technology for resonant tunneling MODFETs and integration of such devices with conventional devices, it is possible that these novel devices might establish a niche in commercial and military applications, even before the scaling limits of conventional complementary metal-oxide semiconductor (CMOS) technology are reached.

**Acknowledgments** This work is the result of a joint collaboration between the groups of Physics and Technology of Optoelectronic Semiconductors at the University of Paderborn, Germany and the Laboratory of Materials, Applications and Environment at the University Mustapha Stambouli of Mascara, Algeria. T.W. and D.J.As. acknowledge financial support by the German Science Foundation (DFG).

## References

- Zado, A., Tschumak, E., Lischka, K., As, D.J.: Electrical characterization of an interface n-type conduction channel in cubic GaN/AlGa<sub>N</sub> heterostructures. *Phys. Status Solidi C* **7**(1), 52–55 (2010)
- Wecker, T., Hörich, F., Feneberg, M., Goldhahn, R., Reuter, D., As, D.J.: Structural and optical properties of MBE-grown asymmetric cubic GaN/Al<sub>x</sub>Ga<sub>1-x</sub>N double quantum wells. *Phys. Status Solidi B* **252**(5), 873–878 (2015)
- Gangwani, P., Pandey, S., Halder, S., Gupta, M., Gupta, R.S.: Polarization dependent analysis of AlGa<sub>N</sub>/Ga<sub>N</sub> HEMT for high power applications. *Solid-state Electron.* **51**(1), 130–135 (2007)
- Bouguenna, Driss, Boudghene Stambouli, A., Mekkakia Maaza, N., Zado, A., As, D.J.: Comparative study on performance of cubic AlGa<sub>N</sub>/Ga<sub>N</sub> nanostructures MODFETs and MOS-MODFETs. *Superlattices Microstruct.* **62**, 260–268 (2013)
- Eller, Brianna S., Yang, Jialing, Nemanich, Robert J.: Electronic surface and dielectric interface states on GaN and AlGa<sub>N</sub>. *J. Vac. Sci. Technol. A* **31**(5), 1–29 (2013)
- Rajan, S., Waltereit, P., Poblenz, C., Heikman, S.J., Green, D.S., Speck, J.S., Mishra, U.K.: Power performance of AlGa<sub>N</sub>/Ga<sub>N</sub> HEMTs grown on SiC by plasma-assisted MBE. *IEEE Electron Dev. Lett.* **25**, 247–249 (2004)
- Haffouz, S., Tang, H., Bardwell, J.A., Hsu, E.M., Webb, J.B., Rolfe, S.: AlGa<sub>N</sub>/Ga<sub>N</sub> field effect transistors with C-doped Ga<sub>N</sub> buffer layer as an electrical isolation template grown by molecular beam epitaxy. *Solid-state Electron.* **49**(5), 802–807 (2005)
- Choi, Y.C., Shi, J., Pophristic, M., Spencer, M.G., Eastman, L.F.: C-doped semi-insulating Ga<sub>N</sub> HFETs on sapphire substrates with a high breakdown voltage and low specific on-resistance. *J. Vac. Sci. Technol. B* **25**(6), 1836–1842 (2007)
- <http://www.wsi.tum.de/nextnano3> and <http://www.nextnano.de>
- Mazumder, P., Kulkarni, S., Bhattacharya, M., Sun, J.P., Haddad, G.I.: Digital circuit applications of resonant tunneling devices. *Proc IEEE* **86**(4), 664–686 (1998)
- Haddad, G.I., Reddy, U.K., Sun, J.P., Mains, R.K.: The bound-state resonant tunneling transistor (BSRTT): fabrication, DC, I-V characteristics and high-frequency properties. *Superlattices Microstruct.* **7**(4), 369–374 (1990)
- Brown, E.R., Soilner, T.C.L.G., Parker, C.D., Goodhue, W.D., Chen, C.L.: Oscillations up to 420 GHz in GaAs/AlAs resonant tunneling diodes. *Appl. Phys. Lett.* **55**(17), 1777 (1989)
- Lunardi, L.M., Sen, S., Capasso, F., Smith, P.R., Sivco, D.L., Cho, A.Y.: Microwave multiple-state resonant tunneling bipolar transistors. *IEEE Electron Dev. Lett.* **10**(5), 219–221 (1989)
- Capasso, F., Sen, S., Beltram, F., Lunardi, L.M., Vengurlekar, A.S., Smith, P.R., Shah, N.J., Malik, R.J., Cho, A.Y.: Quantum functional devices: resonant-tunneling transistors, circuits with reduced complexity, and multiple valued logic. *IEEE Trans. Electron Dev.* **36**(10), 2065–2082 (1989)
- Capasso, F., Mohammed, K., Cho, A.Y.: Resonant tunneling through double barriers, perpendicular quantum transport phenomena in superlattices, and their device applications. *IEEE J. Quantum Electron.* **22**(9), 1853–1869 (1986)
- Chou, S.Y., Allee, D.R., Pease, R.F., Harris, J.S.: Lateral resonant tunneling transistors employing field-induced quantum wells and barriers. *Proc IEEE* **79**(8), 1131–1139 (1991)
- Woodward, T.K., McGill, T.C., Burham, R.D., Chung, H.F.: Resonant tunneling field-effect transistors. *Superlattices Microstruct.* **4**(1), 1–9 (1989)
- Talele, K., Patil, D.S.: Analysis of wave function, energy and transmission coefficients in GaN/AlGa<sub>N</sub> superlattice nanostructures. *Prog. Electromagn. Res.* **81**, 237–252 (2008)
- Birner, S., Schindler, C., Greck, P., Sabathil, M., Vogl, P.: Ballistic quantum transport using the contact block reduction (CBR) method. *J. Comput. Electron.* **8**(3–4), 267–286 (2009)
- Mazumdar, Kaushik, Hussain, Saddam, Singh, Vishwanath Pratap, Ghosal, Aniruddha: Tunneling effect in double barrier nitride (AlGa<sub>N</sub>/Ga<sub>N</sub>) heterostructures at very low temperature. *Sci. Int.* **27**(2), 1017–1019 (2015)
- Lee, Chomsik: Resonant tunneling transistor characteristics using a Fabry–Perot resonator. *J. Korean Phys. Soc.* **31**(1), 112–116 (1997)
- Birner, S., Zibold, T., Andlauer, T., Kubis, T., Sabathil, M., Trelakis, A., Vogl, P.: Nextnano: general purpose 3-D simulations. *IEEE Trans. Electron Dev.* **54**(9), 2137–2142 (2007)
- Hong, H., Shin, M., Vasileska, D., Klimeck, G., Klimeck, G.: Feasibility, accuracy, and performance of contact block reduction method for multi-band simulations of ballistic quantum transport. *J. Appl. Phys.* **111**(6), 063705 (2012)
- Mamaluy, D., Vasileska, D., Sabathil, M., Zibold, T., Vogl, P.: Contact block reduction method for ballistic transport and carrier densities of open nanostructures. *Phys. Rev. B* **71**(24), 245–321 (2005)